Modeling ocean waves and investigation of oceanic wave spectra for wave-to-wire system

DOI : 10.36909/jer.ICEPE.19561

Safdar Rasool*,**, Kashem M. Muttaqi*, Danny Sutanto*, and Shahid Iqbal**

*SECTE, EIS, University of Wollongong, Wollongong, Australia.
**Department of Electrical Engineering, University of Gujrat, Gujrat, Pakistan
Corresponding Author: sr785@uowmail.edu.au

ABSTRACT

The oceanic wave energy is a profuse and sustainable source of clean energy but its enourmous potential is under-exploited. Even though the idea of energy harnessing from oceanic waves is not new, the developments in wave energy conversion technologies are still in an embryonic stage. In most of the studies associated to wave-to-wire systems, oceanic waves are taken as regular waves with a fixed amplitude and a fixed frequency. The main area of focus of the previous studies includes the different conversion stages of the wave-to-wire system, particularly the mechanical, and the electrical conversion stage of the energy and the modeling of oceanic waves for such studies remained neglected in such studies. However, the actual oceanic waves can be presented with the sum of various frequencies to show a specific sea-states with significant wave height and the peak period as the main characterizing parameters. In this study, detailed mathematical modeling of oceanic waves is offered and various wave spectra are investigated for their application in wave-to-wire-based system studies. The best-suited wave spectra are identified parametrically and thereafter it is used for the generation of wave elevation time series in the proposed method presented in this study. The generated time series are appliesd in wave-to-wire systems for the investigation of wave energy conversion devices to mimic the real sea environment. Based on inverse fast Fourier transforms, oceanic wave elevation time series are determined which will be acting as input data for any of the wave energy converters deployed for the capturing

of useable energy.

Keywords: wave spectra; wave energy; wave elevation profile; wave-to-wire system.

INTRODUCTION

Overview of oceanic energy

The oceanic renewable energies have great potential to play a vital role in the world's demand for 100% renewable electricity supply. This sector of renewable energy is progressing with the technological developments enabling the robust operation of offshore devices in a harsh meteorological oceanic environment. The blue energy from the ocean has the ability to meet the global energy demands without any adverse environmental impacts. The ocean alone can act as a more reliable source of electricity when compared with the sun and the wind (Tollefson 2014). The electricity production from the blue energy (tides, currents, temperature and salinity gradients, offshore wind, and wave energy) reached around 42 TWh in 2016 with an installed capacity of 19 GW (Weiss et al. 2018).

Australia is contributing to oceanic energy conversion technologies, and wave energy conversion technology has gained increasing interest. This is reflected by the number of patents filed in the wave energy division as shown in Figure 1.

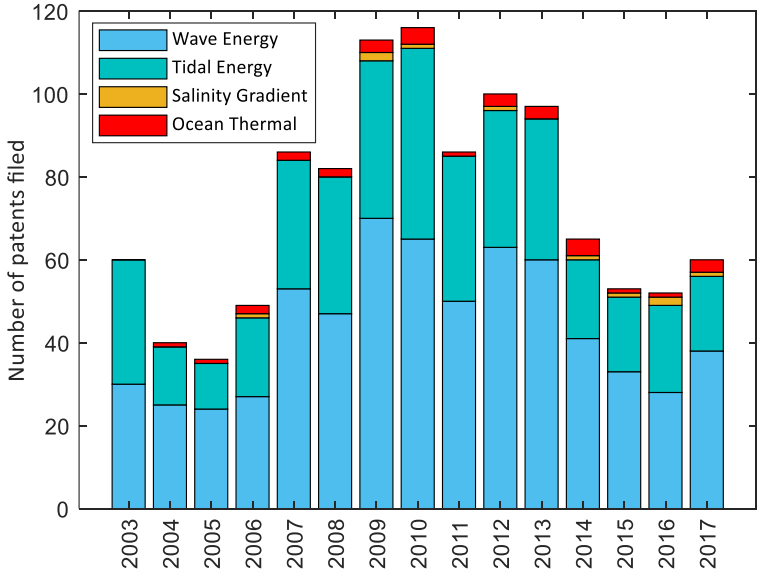

Figure 1. Technological development in oceanic renewables in Australia is reflected by patent evolution (IRENA 2018).

Energy from oceanic waves

The oceanic waves have gigantic untapped potential which can play a pivotal role in the contribution of renewable energy to the increasing power demands. The technical power potential of wave energy is approximately 1 TW along with coastal sites of the world, and this potential can grow up to 10 TW when the potential of the wave energy from open ocean is also included (Melikoglu 2018). This energy amount of energy can meet the world's total energy demand (Rasool et al. 2019). The wave power for different parts of the world is compared in Figure 2. The largest potential for the wave energy in the world based is held by Australia because of its long coastlines (Gunn and Stock-Williams 2012). Detailed studies regarding the development of oceanic wave energy in Australia can be found in (Rasool et al. 2019).

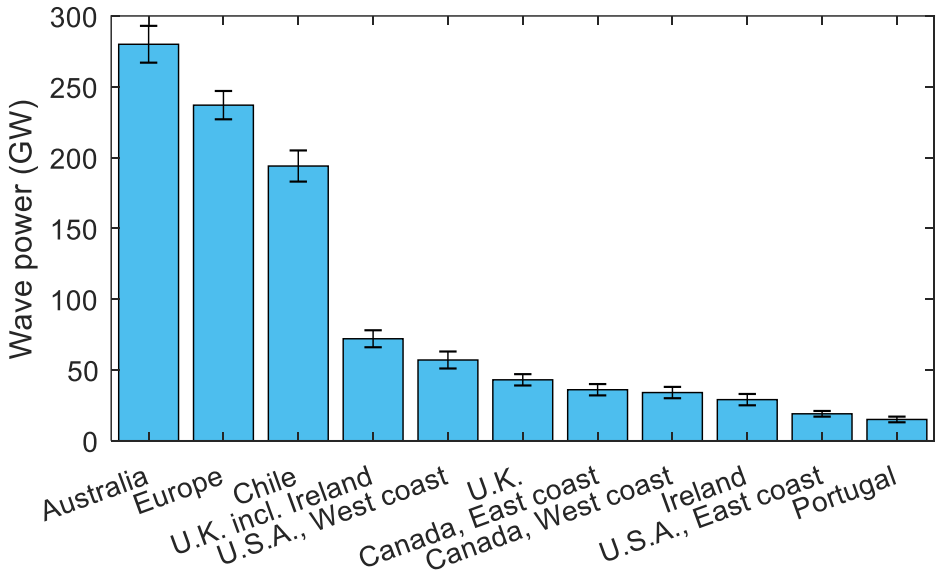

Figure 2. Estimation of wave power in diverse parts of the world.

MODELING OCEANIC WAVES

Linear wave theory

The wave period, the wave height, and the wave direction are seemingly the most related parameters to be investigated at the potential site for the depiction of wave resources. However, there are other parameters as well that are the basis of the linear wave theory (LWT). The LWT is an entrenched theory for the hydrodynamics of waves (Holthuijsen 2007). Although it has some limitations, it provides the basic theoretical rationale for wave modeling. The LWT has the following conventions; (a) the water depth is constant, (b) the wave motion is two dimensional, (c) the waves are time-independent, (d) the water is incompressible, (e) the viscosity, surface tension, and turbulence of the fluid (water) are neglected, (f) the water depth d is large compared to wave height H, and (g) the wavelength L is large compared to wave height H

The velocity potential ($\emptyset$) of waves is LWT is given as (Sheng and Li 2017),

$$\emptyset = \frac{gA \cdot \cosh(k(z+d))}{\omega \cdot \cosh(kd)} \cdot \sin\left(kx - \sqrt{g \cdot k \cdot \tanh(kd)} \cdot t\right) \quad (1)$$

where g is the gravitational constant, A is the amplitude of the wave, d is the depth of water, and k is the wavenumber. The wave propagation direction is along the x-axis and the vertical water level is along the z-axis, x and z represent the respective coordinates in the velocity potential equation. A time series of wave elevation profiles (η) can be approximated as,

$$\eta = A\cos(kx - \sqrt{g \cdot k \cdot \tanh(kd)} \cdot t) \quad (2)$$

A fundamental relation between the wave frequency ω, the wavenumber k, and the water depth d for the linear waves is the dispersion relation. The dispersion relation describes the phase speed for different wavelengths of oceanic waves and the mathematical expression is as,

$$\omega^2 = g \cdot k \cdot \tanh(kd) \quad (3)$$

The phase speed of the oceanic waves varies with the depth of water, and with a constant ω and k, waves will propagate at a quicker phase speed in the deeper water. Similarly, the wavelength L of the ocean waves will also change with the change in the water depth. The relationships for the phase speed, angular frequency, wavelength, and the group velocity are shown in Figure 3. The varying ocean depth, the direction of wave propagation, and the induced waves are represented with a schematic sketch in Figure 3.

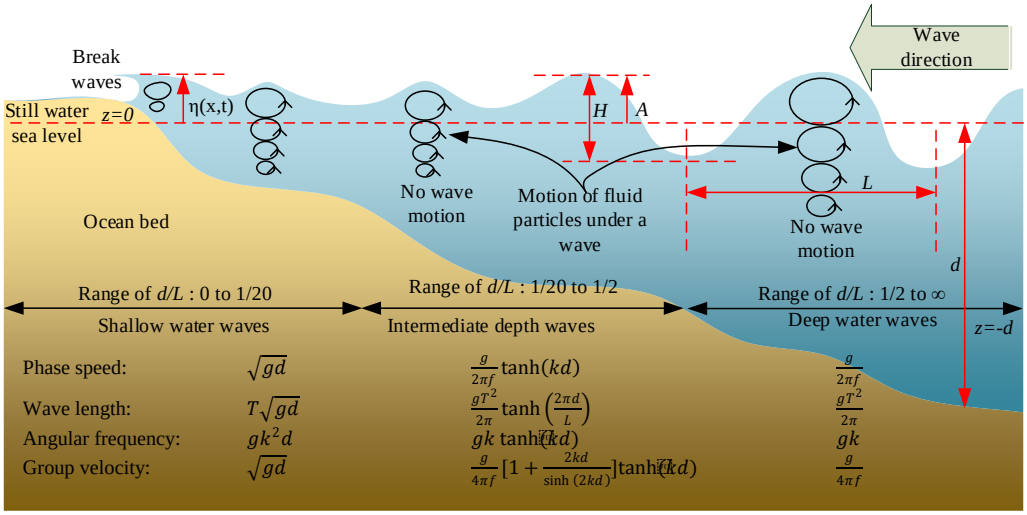

Figure 3. Sketch of oceanic waves representing the prominent wave parameters in the varying depth of water.

Numerical modeling of waves

The modeling of the wave climate in the 3rd generation models is usually presented with the action balance equation. The commonly used wave models are; SWAN (Booij et al. 1999), Mike21-SW (Warren and Bach 1992), WWIII (Tolman 1991), and WAM (Group 1988). The action density is the ratio of the energy density to the wave frequency, and the advantage of the action density quantity over the energy density is its conservation in the presence of oceanic currents. This wave action equation is expressed as;

$$DN/Dt = S/\sigma \tag{4}$$

where N and S are action density spectrum and sources/sinks respectively, and both are

functions of frequency, direction, coordinates, and time. The spectral action balance equation in the SWAN model is described as (Bento et al. 2018);

$$\frac{\partial}{\partial t}N + \frac{\partial}{\partial x}C_x N + \frac{\partial}{\partial y}C_y N + \frac{\partial}{\partial \sigma}C_\sigma N + \frac{\partial}{\partial \theta}C_\theta N = \frac{S(\sigma,\theta,x,y,t)}{\sigma} \quad (5)$$

where C_x and C_y, are the x- and the y- coordinates of propagation velocities, C_θ and C_σ , are the group velocities in the θ- and the σ-space, θ, and σ, are the wave direction and the intrinsic frequency shifting respectively. The changes in the wave spectrum are denoted by $S(\sigma,\theta,x,y,t)$, which is a source term representing all the interactions and the dissipations during the wave propagation as (Amarouche et al. 2020);

$$S(\sigma,\theta,x,y,t) = S_{in} + S_{nl3} + S_{nl4} + S_{ds,w} + S_{ds,b} + S_{ds,br} \quad (6)$$

where S_{in} is the wave growth induced by wind, S_{nl3} and S_{nl4} are the non-linear transfer of wave energy, $S_{ds,w}$ is white capping wave decay, $S_{ds,b}$ is the bottom friction, and $S_{ds,br}$ is the wave breaking due to depth.

Wave power estimation

The transportation of wave energy per unit length of the wavefront can be computed based on the x- and the y- coordinates in the SWAN model. This is the energy transport that is also defined as the wave power flux, usually denoted with J_w.

$$J_w = \sqrt{J_x^2 + J_y^2} \quad (7)$$

where J_x and J_y are defined as (Bento et al. 2018),

$$J_x = \rho g \int_0^{2\pi}\int_0^{\infty} S(f,\theta)\, c_g(f,d) \cos\theta \, df \, d\theta \quad (8)$$

$$J_y = \rho g \int_0^{2\pi}\int_0^{\infty} S(f,\theta)\, c_g(f,d) \cos\theta \, df \, d\theta \quad (9)$$

where ρ is the density of the seawater in kg/m^3, g is gravitational acceleration in m/s^2, f is

wave frequency in 1/s, c_g is the group velocity at which the energy travels for every harmonic component of the wave energy spectrum and $S(f,\theta)$ is the directional wave variance density spectrum showing the energy distribution over different *f* and θ.

Wind-generated waves

In the SWAN model, wind speed at 10m height is used as an input denoted with U_{10}. However, in the computer computations of the SWAN model, the wind-drag coefficient C_D is used to get the friction velocity u_* as (Holthuijsen 2010);

$$u_*^2 = C_D U_{10}^2 \tag{10}$$

where the value of C_D is determined using the empirical relation (Wu 1982),

$$C_D = \begin{cases} 1.2875 \times 10^{-3} & \text{for } U_{10} < 7.5\ m/s \\ (0.8 + 0.065U_{10}) \times 10^{-3} & \text{for } U_{10} \geq 7.5\ m/s \end{cases} \tag{11}$$

The wind-generated waves S_{in} are explained with the help of the feedback mechanism of Miles (Miles 1957) and can be expressed as (Holthuijsen 2010),

$$S_{in}(\sigma,\theta) = \alpha + \beta S(f,\theta) \tag{12}$$

where α is the initial wave growth, and β is the coefficient of exponential growth. The empirical relation developed in (Cavaleri and Rizzoli 1981), is used to calculate α as;

$$\alpha = \begin{cases} \dfrac{1.5 \times 10^{-3}}{2\pi g^2} [u_* \cos(\theta - \theta_{wind})]^4 \exp\left[-\left(\sigma \Big/ \dfrac{0.26\pi g}{28 u_*} \right) \right] & \text{for } |\theta - \theta_{wind}| \leq 90^o \\ 0 & \text{for } |\theta - \theta_{wind}| > 90^o \end{cases} \tag{13}$$

where θ_{wind} is the direction of the wind. The value of β is calculated from the relation (Snyder et al. 1981) as;

$$\beta = max\left\{0, 0.25 \frac{\rho_{air}}{\rho_{water}} \left[28 \frac{u_*}{c} \cos(\theta - \theta_{wind}) - 1 \right] \right\} \sigma \tag{14}$$

where c, ρ_{air}, and ρ_{water} represents the phase speed, air density, and water density respectively.

In actual sea conditions, the waves are omnidirectional and the directional wave energy

spectrum $S(f,\theta)$ can represent the actual sea conditions. However, this becomes computationally expensive, and in more practical cases the unidirectional wave energy spectrum $S(f)$ is used.

The average energy in a unit area of the wave surface can be determined as follows (Wang et al. 2018),

$$E_{avg} = 2\rho g \int_0^\infty S(f)df \tag{15}$$

The wave power flux J_w in terms of $S(f)$ can be approximated as (Rasool et al. 2020),

$$J_w = \rho g \int_0^\infty c_g(f,d) \times S(f)df \tag{16}$$

The value of c_g for any arbitrary depth can be used as (Young 1999),

$$c_g = \frac{g}{4\pi f}\left[1 + \frac{2kd}{\sinh(2kd)}\right]\tanh(kd) \tag{17}$$

Using (16) and (17), the wave power flux J_w can be derived as

$$J_w = \frac{\rho g^2}{4\pi}\int_0^\infty \frac{S(f)}{f}\left[\left(1 + \frac{2k.d}{\sinh(2k.d)}\right)\tanh(k.d)\right]df \tag{18}$$

The parametric wave spectra

The wave spectrum $S(f)$ or $S(\omega)$ is derivable from any of the empirical spectrum formulationsn such as the Torsethaugen, the Scott, the Ochi-Hubble, the TMA, the Liu the Mitsuyasu, the ITTC, the Phillips, the Neumann, the Bretschneider, the Pierson-Moskowitz (PM), or the Joint North Sea Wave Project (JONSWAP). A detailed mathematical description of these spectrums can be found in (Prendergast et al. 2020). However, the most common wave spectra are presented and explained here.

Bretschneider wave spectrum

The Bretschneider wave spectrum $S(f)$ with a peak frequency f_p and significant wave height H_s is given as (Bretschneider 1959),

$$S(f) = \frac{5}{16} H_s^2 f_p^4 f^{-5} \mathrm{e}^{-\left[5f_p^4/4f^4\right]} \tag{19}$$

The Bretschneider spectrum for $H_s = 2,4,6, \text{and } 8m$, and $T_p = 10s$ is shown in Fig. 4(a).

Pierson-Moskowitz wave spectrum

The Pierson-Moskowitz (PM) spectrum with a single input parameter. The single parameter could be significant wave height, wind speed, or the wave peak frequency f_p. The relation can be derived in terms of f_p as (Pierson and Moskowitz 1964),

$$S(f) = \frac{0.0081 g^2 (2\pi)^{-4}}{f^5} \exp\left(-\frac{\left(5/4\right) f_p^4}{f^4}\right) \tag{20}$$

The PM spectrum with $T_p = 6,8,10, \text{and } 12s$ are shown in Fig. 4(b).

Ochi-Hubble wave spectrum

A six parameter spectrum, known as Ochi-Hubble bi-modal spectrum, is presented in (Ochi and Hubble 1977), can be expressed as;

$$S(\omega) = \frac{1}{4} \sum_{i=1,2} \frac{\left(\frac{4\lambda_i + 1}{4} \omega_{pi}^4\right)^{\lambda_i}}{\Gamma(\lambda_i)} \frac{H_{si}}{\omega^{4\lambda_i + 1}} \exp\left(-\frac{4\lambda_i + 1}{4} \left(\frac{\omega_{pi}}{\omega}\right)^4\right) \tag{21}$$

where Γ is the gamma function and all the six parameters can be defined in terms of H_s as: $H_{s1} = 0.84H_s$, $H_{s2} = 0.54H_s$, $\omega_{p1} = 0.70\exp(-0.046H_s)$, $\omega_{p2} = 1.15\exp(-0.039H_s)$, $\lambda_1 = 3,$ and $\lambda_2 = 1.54\exp(-0.062H_s)$. The subscript 1 is for the lower frequency component of the parameter while the subscript 2 is the higher frequency component of the respective parameter. Ochi-Hubble spectrum for $H_s = 2,4,6, \text{and } 8m$ are plotted in Fig. 4(c).

Torsethaugen wave spectrum

A double peak wave spectrum in terms of H_s and T_p is given by Torsethaugen with its empirical relation as (Torsethaugen and Haver 2004),

$$S(f_n) = \sum_{i=1}^{2} (1/16) H_i^2 T_{pi} S_{in}(f_{in}) \tag{22}$$

where

$$S_{1n}(f_{1n}) = 3.26[\{1 + 1.1(\ln\gamma)^{1.19}\}/\gamma] f_{1n}^{-4} e^{-f_{1n}^{-4}} \gamma^{(\exp -(1/2\sigma^2)(f_{1n}-1)^2)} \tag{23a}$$

$$S_{2n}(f_{2n}) = 3.26 f_{2n}^{-4} e^{-f_{2n}^{-4}} \tag{23b}$$

where γ is the peak enhancement factor and σ is between 0.07 to 0.09.

The Torsethaugen spectrum with $H_s = 4m, T_p = 6s; H_s = 6m, T_p = 6s; H_s = 6m, T_p = 8s;$ and $H_s = 8m, T_p = 8s$ is shown in Fig. 4(d).

Wallops wave spectrum

A unified wave spectral model was developed by Huang et al. (Huang et al. 1981), which is known as the Wallops spectrum and its parametric relation is as,

$$S(f) = \frac{\beta g^2}{f^m f_p^{5-m}} \exp\left(-\frac{m}{4}(f_p/f)^4\right) \tag{24}$$

where β is the internal parameter and m is defined as,

$$m = \left|\frac{\log(2/Ak)^2}{\log(0.5)}\right| \tag{25}$$

The Wallop spectrum with $T_p = 6\ s$ and $m = 3,4,5,6$ are shown in Fig. 4(e).

TMA wave spectrum

The TMA spectrum is used to define the wind-generated waves in a limited depth of water. The parametric spectral form is given by (Bouws et al. 1985),

$$S(\omega) = \alpha g^2 \frac{1}{\omega^5} \exp\left(-\frac{5}{4}\frac{\omega_p^4}{\omega^4}\right) \gamma^{\exp\left[-\frac{(\omega-\omega_p)^2}{2\omega_p^2\sigma^2}\right]} \left[\frac{k_h^{-3}\frac{\partial k_h}{\partial \omega}}{2g^2\omega^{-5}}\right] \tag{26}$$

where $\alpha = 0.0081$ and $k_h$is approximated using numerical methods.

The TMA spectrum with $H_s = 4m, T_p = 8s; H_s = 5m, T_p = 10s; H_s = 6m, T_p =$

$12s$; and $H_s = 7m, T_p = 14s$ is shown in Fig. 4(f).

JONSWAP wave spectrum

The most common and the generalized wave spectrum is the JONSWAP spectrum (Sheng 2019) and its parametric relation is as,

$$S(f) = \frac{5(1 - 0.29\ln(\gamma))}{16} H_s^2 \frac{f_p^4}{f^5} \exp\left(-\frac{5}{4}\frac{f_p^4}{f^4}\right) \gamma^{\exp\left[-\frac{(f-f_p)^2}{2f_p^2\sigma^2}\right]} \quad (27)$$

where $\sigma = 0.07$ for $f \leq f_p$, $\sigma = 0.09$ for $f \geq f_p$ and γ is the Weibull location parameter also known as the peakness factor. The PM, the Bretschneider, the Wallops, and the TMA spectrum can also be derived from Equation(27) by varying γ and m values. The JONSWAP spectrum with $H_s = 4m, T_p = 10s,$ and $\gamma = 2,3,4,5$ are shown in Fig. 4(g).

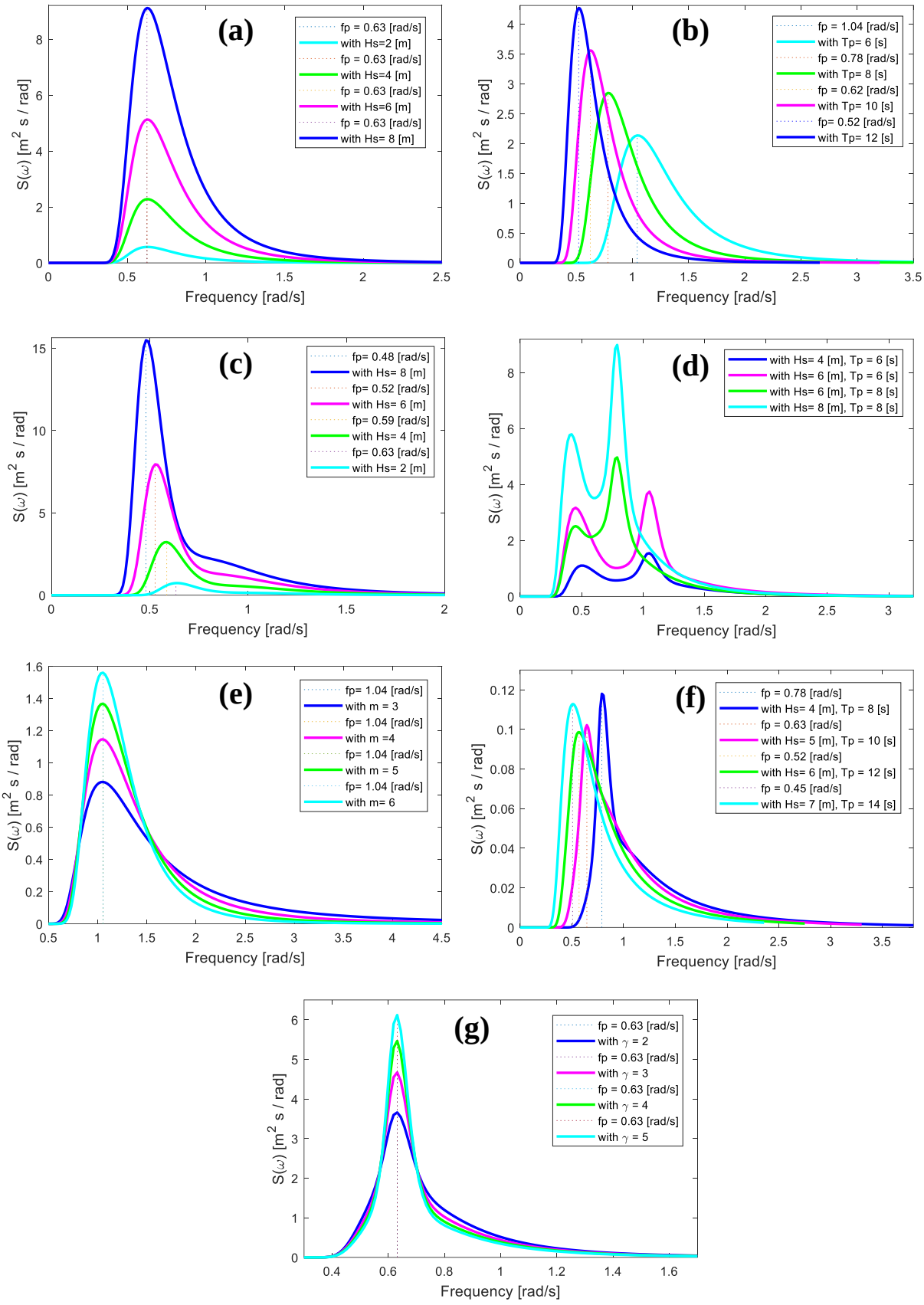

Figure 4. (a) Bretschneider, (b) Pierson-Moskowitz, (c) Ochi-Hubble, (d) Torsethaugen, (e)

Wallops, (f) TMA, and (g) JONSWAP spectra.

OCEANIC WAVE SPECTRA APPLICATION IN WAVE-TO-WIRE SYSTEMS

The energy content or the spectral density of a wave with a particular frequency is predictable from the shape of the spectrum. The JONSWAP spectrum has a sharp shape with a narrow area, as shown in Figure 4; this specifies that most of the energy lies within a limited band when compared with other types of spectra. This characterizes a seamless fetch-limited condition obtained via parametric observation. Therefore, a JONSWAP spectrum is suitable for engineering applications specifically for wave-to-wire systems. Applying the inverse fast Fourier transform on the JONSWAP spectrum, wave elevation profiles are generated for 200 s, as shown in Figure 5. These wave profiles can present the actual oceanic waves by showing the same signal power spectral density and can serve as an input to wave-to-wire systems for further investigation of the wave energy conversion schemes for harnessing the energy.

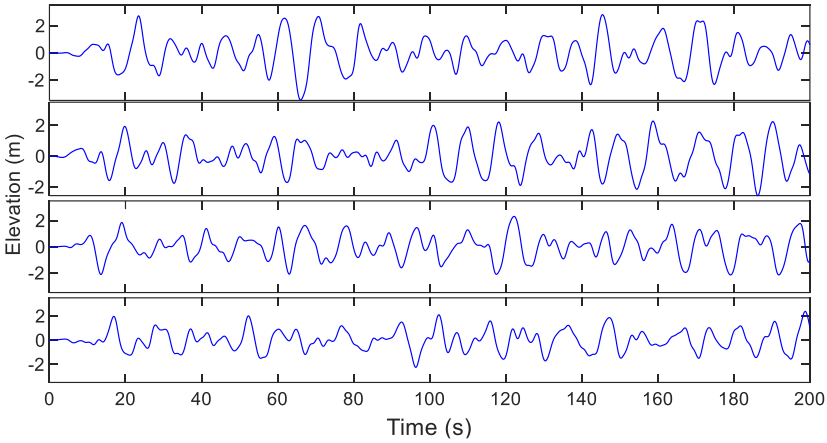

Figure 5. The obtained wave elevation profile for 200 s duration for $\gamma = 5,4,3,$ and 2**.**

CONCLUSION

In this study, detailed modeling of oceanic waves is presented. The modeling of oceanic waves is particularly presented from the perspective of wave energy conversion technology. Thereafter, various wave spectra are monitored parametrically through MATLAB. The JONSWAP spectrum is identified as the most suited spectrum based on the limited fetch which is ideal for wave-to-wire systems. Based on the inverse fast Fourier transform, wave

elevation profiles are acquired which are used as irregular waves for the wave-to-wire systems.

ACKNOWLEDGEMENTS

The authors would like to acknowledge the financial support for Ph.D. studies of the corresponding author (Safdar Rasool) from the University of Gujrat, Pakistan, and the University of Wollongong, Australia.

REFERENCES

Amarouche, K., Akpınar, A., Bachari, N. E. I., & Houma, F. 2020. "Wave energy resource assessment along the Algerian coast based on 39-year wave hindcast." Renewable Energy, 153, 840–860.

Bento, A. R., Martinho, P., & Guedes Soares, C. 2018. "Wave energy assessement for Northern Spain from a 33-year hindcast." Renewable Energy, 127, 322–333.

Booij, N., Ris, R. C., & Holthuijsen, L. H. 1999. "A third-generation wave model for coastal regions: 1. Model description and validation." Journal of Geophysical Research: Oceans, 104(C4), 7649–7666.

Bouws, E., Günther, H., Rosenthal, W., & Vincent, C. L. 1985. "Similarity of the wind wave spectrum in finite depth water: 1. Spectral form." Journal of Geophysical Research, 90(C1), 975.

Bretschneider, C. L. 1959. Wave variability and wave spectra for wind-generated gravity waves. The Board.

Cavaleri, L., & Rizzoli, P. M. 1981. "Wind wave prediction in shallow water: Theory and applications." Journal of Geophysical Research, 86(C11), 10961.

Group, T. W. 1988. "The WAM Model—A Third Generation Ocean Wave Prediction Model." Journal of Physical Oceanography, 18(12), 1775–1810.

Gunn, K., & Stock-Williams, C. 2012. "Quantifying the global wave power resource."

Renewable Energy, Elsevier Ltd, 44, 296–304.

Holthuijsen, L. H. 2007. Waves in oceanic and coastal waters. Waves in Oceanic and Coastal Waters.

Holthuijsen, L. H. 2010. Waves in oceanic and coastal waters. Cambridge university press.

Huang, N. E., Long, S. R., Tung, C.-C., Yuen, Y., & Bliven, L. F. 1981. "A unified two-parameter wave spectral model for a general sea state." Journal of Fluid Mechanics, 112(1), 203.

IRENA. 2018. "RE Technology Patents Reports." <http://inspire.irena.org/Pages/patents/Patents-Search.aspx> (Dec. 1, 2020).

Melikoglu, M. 2018. "Current status and future of ocean energy sources: A global review." Ocean Engineering, 148, 563–573.

Miles, J. W. 1957. "On the generation of surface waves by shear flows." Journal of Fluid Mechanics, 3(02), 185.

Ochi, M. K., & Hubble, E. N. 1977. "Six-parameter wave spectra." Coastal Engineering 1976, 301–328.

Pierson, W. J., & Moskowitz, L. 1964. "A proposed spectral form for fully developed wind seas based on the similarity theory of S. A. Kitaigorodskii." Journal of Geophysical Research, 69(24), 5181–5190.

Prendergast, J., Li, M., & Sheng, W. 2020. "A Study on the Effects of Wave Spectra on Wave Energy Conversions." IEEE Journal of Oceanic Engineering, 45(1), 271–283.

Rasool, S., Islam, M. R., Muttaqi, K. M., & Sutanto, D. 2019. "The Grid Connection of Linear Machine-Based Wave Power Generators." Advanced Linear Machines and Drive Systems, Springer Singapore, Singapore, 303–341.

Rasool, S., Muttaqi, K. M., & Sutanto, D. 2020. "Modelling of a wave-to-wire system for a wave farm and its response analysis against power quality and grid codes." Renewable

Energy, 162, 2041–2055.

Sheng, W. 2019. "Power performance of BBDB OWC wave energy converters." Renewable Energy, 132, 709–722.

Sheng, W., & Li, H. 2017. "A Method for Energy and Resource Assessment of Waves in Finite Water Depths." Energies, 10(4), 460.

Snyder, R. L., Dobson, F. W., Elliott, J. A., & Long, R. B. 1981. "Array measurements of atmospheric pressure fluctuations above surface gravity waves." Journal of Fluid Mechanics, 102, 1–59.

Tollefson, J. 2014. "Power from the oceans: Blue energy." Nature, 508(7496), 302–304.

Tolman, H. L. 1991. "A Third-Generation Model for Wind Waves on Slowly Varying, Unsteady, and Inhomogeneous Depths and Currents." Journal of Physical Oceanography, 21(6), 782–797.

Torsethaugen, K., & Haver, S. 2004. "Simplified double peak spectral model for ocean waves." Proceedings of the Fourteenth International Offshore and Polar Engineering Conference, Toulon, France, 23–28.

Wang, L., Isberg, J., & Tedeschi, E. 2018. "Review of control strategies for wave energy conversion systems and their validation: the wave-to-wire approach." Renewable and Sustainable Energy Reviews, 81, 366–379.

Warren, I. R., & Bach, H. K. 1992. "MIKE 21: a modelling system for estuaries, coastal waters and seas." Environmental Software, 7(4), 229–240.

Weiss, C. V. C., Guanche, R., Ondiviela, B., Castellanos, O. F., & Juanes, J. 2018. "Marine renewable energy potential: A global perspective for offshore wind and wave exploitation." Energy Conversion and Management, 177, 43–54.

Wu, J. 1982. "Wind-stress coefficients over sea surface from breeze to hurricane." Journal of Geophysical Research, 87(C12), 9704.

Young, I. R. 1999. Wind generated ocean waves. Elsevier.